Quenching and excitation-transfer processes in the $n=4$ helium sublevels in a low-pressure glow discharge

A. Catherinot and B. Dubreuil
Groupe de Recherches sur l'Energétique des Milieux Ionisés, Université d'Orléans, 45046 Orleans Cedex, France
(Received 11 July 1980)

Collisional and radiative processes in a glow discharge leading to quenching and excitation transfer in the $n=4$ helium sublevels are investigated by means of a laser-perturbation method. Laser-induced population perturbations are solutions of coupled rate equations, the coefficients of which are determined by an accurate numerical method of data analysis (the identification method) previously developed, so as to minimize the difference between experimental curves and those calculated from the model. In the pressure and current-intensity ranges investigated, only the radiative and atom-atom collision processes contribute to quenching and excitation transfer in the $n=4$ sublevels. Numerical identification of the $n=4$ experiments provides a nearly complete set of thermally averaged cross sections and in particular shows that the singlet-triplet transfers are mainly due to stepwise collisional processes via the $4F$ state.

I. INTRODUCTION

In two previous papers dealing with quenching and excitation-transfer processes in the $n=3$ helium sublevels[1] and excitation-transfer mechanisms within the 3^3D helium level fine structure,[2] henceforth, respectively, referred to as I and II, we have demonstrated that a time-resolved laser-perturbation technique associated with an efficient numerical method of data analysis (the identification method) can lead to the accurate determination of collisional- and radiative-rate coefficients in a weakly ionized gas.

In this paper, the same procedure is applied to the study of quenching and excitation-transfer mechanisms in the $n=4$ helium sublevels produced in the positive column of a low-pressure, low-current helium glow discharge. Despite numerous experimental investigations both in helium-electron-beam-interaction experiments[3-5] and by means of selective time-resolved laser-perturbation techniques,[6-8] some questions are still open, particularly those concerning the orbital quantum number selection rules and the singlet-triplet excitation transfers in atom-atom binary encounters. These latter processes, in apparent contradiction to the Wigner spin conservation rules,[9] were first observed in 1932 by Lees *et al.*[10] in an investigation of the helium emission spectrum induced by electron impact and more recently improved by Maurer *et al.*[11] and St John *et al.*[12] In order to explain these unexpected experimental results, according to the Wigner spin conservation rules, Lin *et al.*[13] propose that singlet-triplet transfers may be ascribed to two-step processes of the type

$$\mathrm{He}(4\,^1D)+\mathrm{He}(1\,^1S)\rightarrow\mathrm{He}(4F)+\mathrm{He}(1\,^1S)$$

followed by

$$\mathrm{He}(4F)+\mathrm{He}(1\,^1S)\rightarrow\mathrm{He}(4\,^3D)+\mathrm{He}(1\,^1S) \quad (1)$$

or

$$\mathrm{He}(4F)\rightarrow\mathrm{He}(3\,^3D)+h\nu\,,$$

owing to the fact that the spin-orbit approximation is not valid for He I (neutral helium) levels whose orbital quantum numbers are larger than three. The experimental study of Abrams *et al.*[14] in a helium discharge by means of a selective perturbation method, and the theoretical calculations performed by Van den Eynde *et al.*[15] tend to support the validity of this reaction scheme. Indeed, in Ref. 15, calculating the Breit-Pauli Hamiltonian matrix elements and the singlet-triplet mixing coefficients of He I excited states, the authors show that the $4F$ helium state wave function ϕ_{4F} can be written

$$\phi_{4F}=a_{\text{singlet}}\,\phi_{4\,^1F}+a_{\text{triplet}}\,\phi_{4\,^3F}\,,$$

with

$$a_{\text{singlet}}/a_{\text{triplet}}=0.593\,.$$

Then the $4\,^1F$ and $4\,^3F$ sublevels are largely mixed and henceforth the $4F$ state will be considered as a whole.

II. POPULATION RATE EQUATIONS

The excited-state population relaxations that follow a short (compared to the typical excited-state lifetimes) and selective optical pumping in a stationary low-pressure, low-current helium glow discharge have been widely studied in paper I. Let us just recall that if the $|b\rangle\rightarrow|a\rangle$ transition is pumped by a laser pulse, the population variations $\Delta N_i(t)$ of the $n+1$ effectively perturbed levels can be described in the laser-free regime by the

"perturbed" rate equations:

$$\frac{d\Delta N_i}{dt} = -\Delta N_i\left(\sum_{k<i} A_{ik}\Lambda_{ik} + n_a\sum_{k\neq i} R_{ik} + n_e\sum_{k\neq i} S_{ik}\right) + \sum_{j\neq i}\Delta N_j(A_{ji}\Lambda_{ji} + n_a R_{ji} + n_e S_{ji}),$$
$$\Delta N_i(t_0) = \Delta N_i^0, \quad i,j = 1,2,\ldots,n+1. \tag{2}$$

In Eq. (2), the same notations as in paper I are used. Particularly the following mechanisms have been taken into account:

spontaneous emission of radiation (Λ_{ij}, optical escape factor)

$$|i\rangle \xrightarrow{A_{ij}\Lambda_{ij}} |j\rangle + h\nu_{ij}, \tag{3}$$

atom-atom collisional excitation transfer

$$|i\rangle + |\text{ground state}\rangle \xrightarrow{R_{ij}} |j\rangle + |\text{ground state}\rangle + \Delta E_{ij}, \tag{4}$$

electron-atom inelastic collisions

$$|i\rangle + \bar{e} \xrightarrow{S_{ij}} |j\rangle + \bar{e} + \Delta E_{ij}. \tag{5}$$

n_a and n_e are, respectively, the atomic ground state and electronic population densities. In the laser-free relaxation regime, the elementary processes starting from $|b\rangle$ to populate the $|i\rangle$ states can be entirely neglected and the $|b\rangle$ state just acts as a population "reservoir". Then, one can remove the $|b\rangle$ state population equation (2) in the system which becomes

$$\frac{d\Delta\vec{N}}{dt} = A\Delta\vec{N}, \quad \Delta N(t_0) = \Delta N^0, \tag{6}$$

$$\Delta N_b(t) = \sum_{i=1}^{n}\Delta N_i(t) + \xi(t), \tag{7}$$

where A is a square matrix of order n, $\Delta\vec{N}(t)$ being the perturbed population state vector at time t. Equation (7) expresses conservation of the particle number at each time when $\xi(t)$ represents the population losses induced from states $|i\rangle$ on states $|k\rangle \neq |j\rangle$, the populations of which do not intervene explicitly in Eq. (2). In Eq. (6), an element $a_{ij}(i \neq j)$ of the matrix A represents the coefficient of reactions leading to the formation of state $|i\rangle$ from state $|j\rangle$. This element is positive and, as in paper I, can be generally written

$$a_{ij} = \alpha_{ij} + \sum_{\phi}\beta_{ij}^{\phi}\phi, \tag{8}$$

where α_{ij} is the spontaneous transition coefficient $|j\rangle \rightarrow |i\rangle$ (radiative transition) and β_{ij}^{ϕ} is the $|j\rangle \rightarrow |i\rangle$ transfer reaction rate induced by a process characterized by the physical quantity ϕ (n_a, n_e, for example). The diagonal element a_{ii} is negative and corresponds to the total destruction rate coefficient of state $|i\rangle$. Generally, a_{ii} is given as

$$a_{ii} = -a_{ki} - \sum_{j=1, j\neq i}^{n} a_{ji}, \tag{9}$$

where a_{ki} represents the population loss from state $|i\rangle$ outside the n-state "perturbed system" described by Eq. (6) (diffusion, associative ionization, etc,). Using the Eq. (8), the matrix A may be written

$$A = \alpha + \sum_{\phi}\beta^{\phi}\phi, \tag{10}$$

where $\alpha = \{\alpha_{ij}\}$ and $\beta^{\phi} = \{\beta_{ij}^{\phi}\}$ are square matrix of order n and ϕ are determined by the experimental conditions: Gas pressure and temperature, and discharge current intensity. As in I and II, the problem now is to identify α and β from measurements of the $\Delta N_i(t)$. The relaxation matrix A is determined so as to minimize the difference between the experimental values of $\Delta N_i(t)$ and the ones calculated from the model by means of the numerical identification method widely described in Refs. 1, 2, 16, and 17.

III. EXPERIMENTAL SETUP

The experimental setup was described in previous papers dealing with collisional and radiative processes in helium,[1,2,16-19] hydrogen,[20] argon,[21] and nitrogen[22] glow discharges. Let us just recall the essential features of the experiment. The excited helium states are populated in a capillary glow discharge with pressure and current-intensity ranges respectively: $0.1 < P < 4$ Torr, and $10 < i < 50$ mA. The other characteristics of the discharge are the same as in paper I and in paper II: Electronic density $10^{10} < n_e < 10^{11}$ cm^{-3}, electronic mean kinetic energy $3 < E_e < 20$ eV, and gas temperature $T_g = 340 \pm 5$ K. A tunable dye laser excited by a nitrogen laser (energy/pulse < 10 μJ, pulse width ~ 4 ns, spectral width ~ 0.2 Å) is used to induce a population variation on a selected $n = 4$ helium sublevel by optical pumping. The discharge is longitudinally traversed by the laser beam and the fluorescence light emitted by a cross section of the positive column is observed by means of a 2-meter grating spectrometer and a photomuliplier tube. Time dependence of the fluorescence light intensity is analyzed by means of a Princeton Applied Research boxcar averager PAR 162 (time resolution = 5 ns) connected to a Data General minicomputer (Nova 3). Calibration of the system is achieved by means of a tungsten-ribbon filament lamp.[16,17] In fact, due to the linearity of Eq. (2), only a relative calibration is needed.

IV. MEASUREMENTS AND SIMPLIFICATION OF EQ. (6)

A. Measurements

A partial diagram of the $n = 2$, 3, and 4 He I

atomic energy states is shown in Fig. 1. Perturbing the population of one $n=4$ He I sublevel by selective laser optical pumping of one of the five transitions:

$4\,^1D$: $2\,^1P$-$4\,^1D$, $\lambda=4922$ Å, laser dye C 500,

$4\,^1P$: $2\,^1S$-$4\,^1P$, $\lambda=3964$ Å, laser dye PBBO,

$4\,^3D$: $2\,^3P$-$4\,^3D$, $\lambda=4471$ Å, laser dye 7D4MC,

$4\,^1S$: $2\,^1P$-$4\,^1S$, $\lambda=5047$ Å, laser dye C 500,

$4\,^3S$: $2\,^3P$-$4\,^3S$, $\lambda=4713$ Å, laser dye C 102. (11)

We have systematically investigated all the $n=3$, 4, and 5 sublevels observable with our detection system, on which population variations $\Delta N_i(t)$ may be induced by collisional or radiative coupling with the laser perturbed sublevel. The $\Delta N_i(t)$ are deduced from the time-resolved analysis of the fluorescence light intensity variations. No population perturbation on any $n=5$ sublevel is observed when one of the transitions (11) is pumped in all the experimental situations (P, i) we have studied. In the same way, as reported in paper I (see also Refs. 16, 17, and 19), no population variation is induced on any $n=4$ sublevel when one $n=3$ sublevel population is perturbed. These important results can be explained by the ineffective contributions of reactions (4) and (5) respectively due to the large energy gap between $n=3$, 4, and 5 helium states compared to the mean kinetic energy of atoms ($\Delta E_{3,4} > 20kT_g$, $\Delta E_{4,5} > 10kT_g$) and to the low electronic density in the discharge ($n_e < 10^{11}$ cm^{-3}). In fact, when one of the three first transitions (11) is pumped, fluorescence light is only detected originating from the $4\,^1S$, $4\,^1P$, $4\,^1D$, $3\,^1P$, and $3\,^1D$ singlet states, and $4\,^3S$, $4\,^3P$, $4\,^3D$, $3\,^3P$, and $3\,^3D$ triplet states. The population of the $4F$ state is also obviously perturbed but cannot be directly observed, the $4\,^1F$-$3\,^1D$ and $4\,^3F$-$3\,^3D$ radiative transitions ($\lambda \sim 1.87$ μm) lying out the spectral range of our detection system. When the population of the $4\,^1S$ or $4\,^3S$ state is perturbed, weak excitation transfers are only detected for the higher pressure values we have studied, respectively on the $4\,^1D$ state and on the $4\,^3D$ and $4\,^3P$ states. Note that the $4\,^3P$ and $4F$ states cannot be directly perturbed by laser excitation, since all the radiative transitions starting from these states lie out the pulsed dye-laser spectral range.

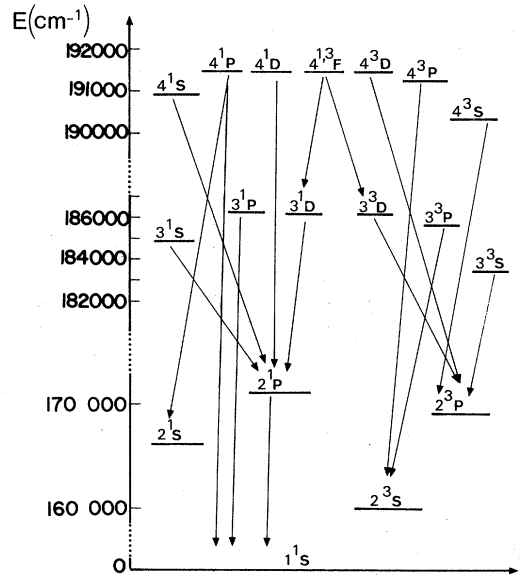

FIG. 1. Partial energy diagram of helium excited atomic states involved in the experiment.

On the other hand, recording profiles of spectral lines starting from the states under study indicate that radiation trapping is negligible excepted for the resonant lines: $\Lambda_{ij}=1$ for $i \neq 3\,^1P$, and $4\,^1P$ and $j \neq 1\,^1S$; $\Lambda_{3^1P-1^1S} \neq 1$ and $\Lambda_{4^1P-1^1S} \neq 1$. For each of the five pumping experiments (11) the population relaxations $\Delta N_i(t)$ of the "perturbed states" have been studied for various discharge conditions, yielding five independent sets of experimental data.

B. Simplification of Eq. (6)

The qualitative observations of Sec. IV A lead to important simplifications in Eq. (6). On one hand, we can deduce that the "perturbed system" of Sec. II is limited to the eleven states: $4\,^1S$, $4\,^1P$, $4\,^1D$, $4F$, $4\,^3D$, $4\,^3P$, $4\,^3S$, $3\,^1D$, $3\,^1P$, $3\,^3D$, and $3\,^3P$. Equation (6) describing the evolution of this "eleven-states perturbed system" is written in matrix form in Fig. 2. On the other hand, as discussed in Sec. IV A, the contributions of the reactions

$$\mathrm{He}(3^{2S+1}L) + \mathrm{He} \rightarrow \mathrm{He}(4^{2S'+1}L') + \mathrm{He}, \quad (12)$$

$$\mathrm{He}(3^{2S+1}L) + \bar{e} \rightarrow \mathrm{He}(4^{2S'+1}L') + \bar{e}, \quad (13)$$

are negligibly small for our experimental conditions and the corresponding coefficients in the A matrix vanish (dashed zone in Fig. 2). Then Eq. (6) may be dissociated into two subsystems describing, respectively, the population relaxations of the $n=4$ and of the $n=3$ sublevels. Moreover the former can be solved independently of the latter. In fact, measurements show that the couplings between the $n=4$ and $n=3$ subsystems are essentially due to spontaneous radiative transitions. These processes are submitted to well-known selection rules leading to supplementary simplifications in the $n=3$ subsystem; the underlined coefficients in Fig. 2 vanish.

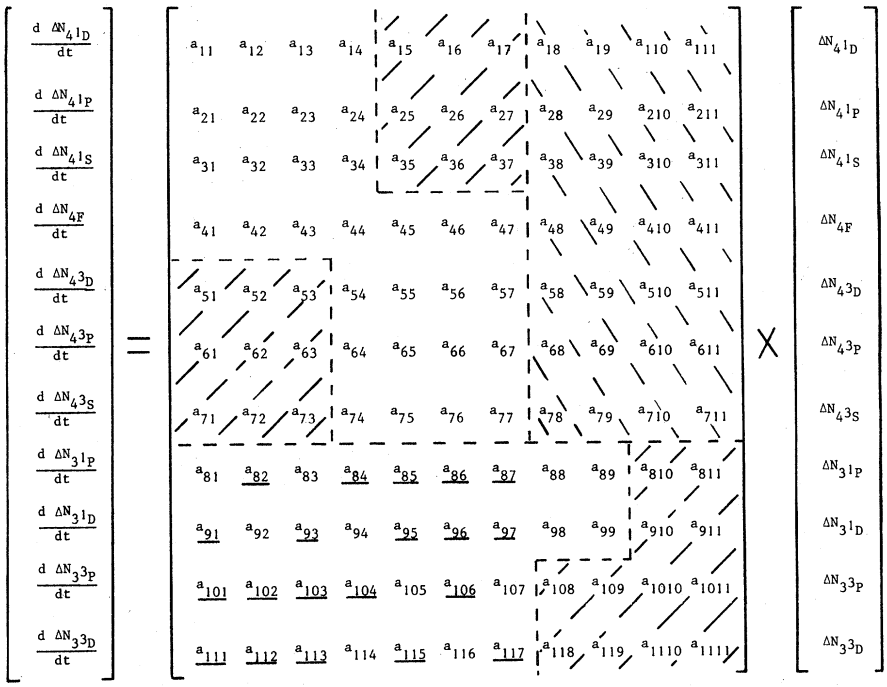

FIG. 2. Relaxation equations, in matrix form, of the eleven-state perturbed system. (See text Sec. IV B).

If we assume that singlet-triplet excitation transfers between sublevels of orbital quantum number $L < 3$ are negligible (dashed zone in Fig. 2), the A matrix still simplifies and the system of Fig. 2 can be solved by blocks. As reported in paper I, this last assumption agrees well with the experimental results for the $n=3$ helium sublevels. In the first numerical identifications, the whole $n=4$ subsystem was identified to the measured relaxation curves $\Delta N_i(t)$ for various experimental situations (P, i). In all cases, the singlet-triplet coupling coefficients between $(n=4,\ L<3)$ sublevels were found negligibly small and the following conclusions hold: According to Wigner spin conservation rules, the contributions of reactions

$$\mathrm{He}(4^{2S+1}, L<3)+\mathrm{He}\rightarrow \mathrm{He}(4^{2S'+1}, L<3)+\mathrm{He}, \quad S\neq S' \tag{14}$$

are negligible and excitation transfers by electronic inelastic collisions

$$\mathrm{He}(4^{2S+1}, L<3)+\bar{e}\rightarrow \mathrm{He}(4^{2S'+1}, L'<3)+\bar{e}, \quad S\neq S' \tag{15}$$

are inefficient in our experimental conditions.

In the next calculations, these coefficients were henceforth cancelled yielding a substantial gain in computational time.

C. Determination of $\Delta N_{4F}(t)$

While the $\Delta N_i(t)$ $(|i\rangle \neq 4F)$ can be deduced from measurements of the corresponding variation of fluorescence light intensity, as previously quoted in Sec. IV A. $\Delta N_{4F}(t)$ is not directly attainable with our experimental device. However, $\Delta N_{4F}(t)$ can be deduced from experimental values of $\Delta N_{3^3D}(t)$. Indeed, taking into account the simplification of Sec. IV B, the eleventh equation in Fig. 2 can be written[17,19] as:

$$\frac{d\Delta N_{3^3D}}{dt} = A_{4\,^3F-3\,^3D}\Delta N_{4\,^3F} + A_{4\,^3P-3\,^3D}\Delta N_{4\,^3P} + (n_a R_{3\,^3P-3\,^3D} + n_e S_{3\,^3P-3\,^3D})\Delta N_{3\,^3P}$$
$$+ (n_a R_{3\,^3S-3\,^3D} + n_e S_{3\,^3S-3\,^3D})\Delta N_{3\,^3S} - \Gamma_{3\,^3D}\Delta N_{3\,^3D}, \tag{16}$$

where Γ_{3^3D} represents the total quenching rate coefficient of the $3\,^3D$ state. As reported in paper I for the same experimental conditions, no excitation transfers induced by electronic collisions have been observed and the excitation transfers $3\,^3P \rightarrow 3\,^3D$ and $3\,^3S \rightarrow 3\,^3D$ have been found very small $(\bar{\sigma}_{3^3P-3^3D} = 0.15 \pm 0.1\ \text{Å}^2,\ \bar{\sigma}_{3^3S-3^3D} < 0.1\ \text{Å}^2)$ so that these contributions in Eq. (16) are at least two

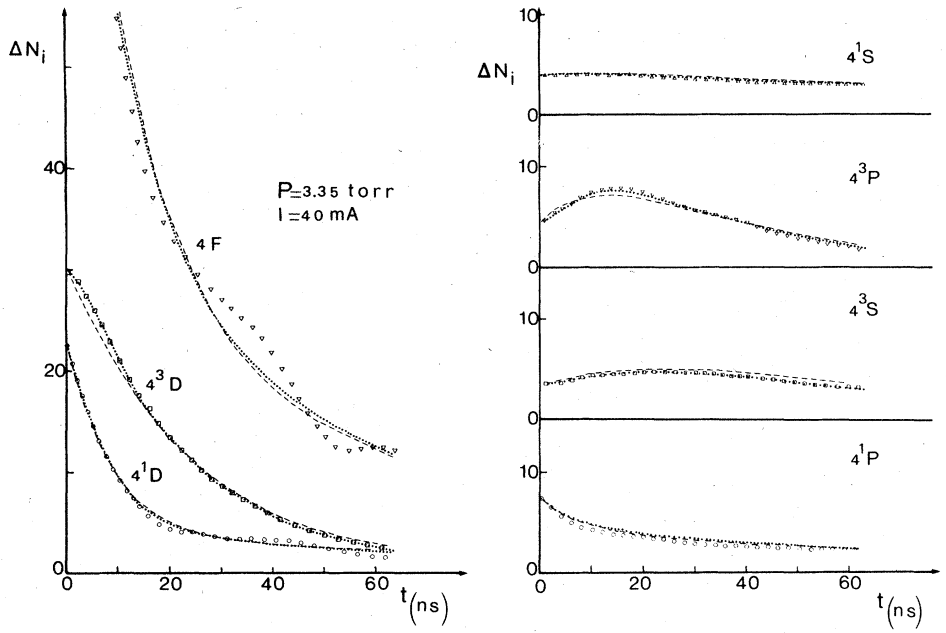

FIG. 3. Comparison between experimental relaxation curves $\Delta N_i(t)$ and "identified" ones for $P = 3.35$ Torr and $i = 40$ mA; the $2\,^1P$-$4\,^1D$ transition is optically pumped (arbitrary units); □▽○ experimental results; ····· identification error = 7.0%, 600 iterations; - - - - - identification error = 6.4%, 600 iterations.

orders of magnitude lower than the others. Furthermore, $A_{4^3P-3^3D}(\sim 0.277\ 10^7\ s^{-1}) \ll A_{4^3F-3^3D}$ $(\sim 1.3\ 10^7\ s^{-1})$[1,23] and $\Delta N_{4\,^3F}$ (statistical weight $= 21$) is always larger than $\Delta N_{4\,^3P}$ (statistical weight $= 9$).[24] Then Eq. (16) may be written to a rather good approximation as:

$$\frac{d\Delta N_{3^3D}}{dt} \simeq A_{4^3F-3^3D}\Delta N_{4F} - \Gamma_{3^3D}\Delta N_{3^3D}\,. \qquad (17)$$

Γ_{3^3D} is a function of helium pressure and has been measured in paper I. Then for a given experimental situation, the population relaxation $\Delta N_{4F}(t)$ can be deduced from the measured $\Delta N_{3^3D}(t)$ through the relation

$$\Delta N_{4F}(t) \simeq \frac{4}{3}\frac{1}{A_{4^3F-3^3D}}\left(\frac{d\Delta N_{3^3D}}{dt} + \Gamma_{3^3D}\Delta N_{3^3D}\right). \qquad (18)$$

Note that in Eq. (18) the evaluation of the term $d\Delta N_{3^3D}/dt$ from the experimental curve ΔN_{3^3D} is needed. Despite least square calculations of $d\Delta N_{3^3D}/dt$, the experimental noise on $\Delta N_{3^3D}(t)$ leads to small numerical instabilities yielding "oscillations" on the calculated $\Delta N_{4F}(t)$ curve, as one can observe in Fig. 3 and in Fig. 4.

V. EXPERIMENTAL RESULTS AND NUMERICAL IDENTIFICATION

A. $4\,^1D$, $4\,^1P$, and $4\,^3D$ state population perturbations

For each of these three experiments, the $n = 4$

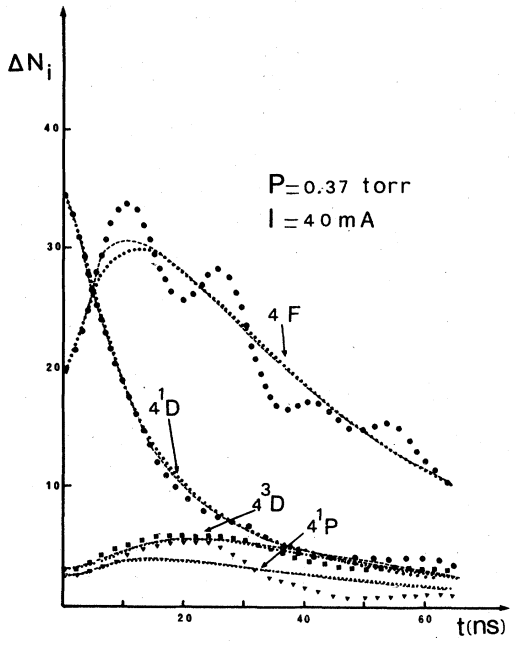

FIG. 4. Comparison between experimental relaxation curves $\Delta N_i(t)$ and identified ones for $P = 0.37$ Torr and and $i = 40$ mA; the $2\,^1P$-$4\,^1D$ transition is optically pumped (arbitrary units); ■●▼ experimental results; ····· identification error = 9.1%, 600 iterations; - - - - - identification error = 9.8%, 600 iterations. At this pressure value, excitation transfers on the $4\,^3P$, $4\,^3S$, and $4\,^1S$ states are not detected experimentally.

subsystem of Fig. 2 is identified to the experimental relaxation curves $\Delta N_i(t)$ for various pressure values P in the 0.3–4 Torr range and for two discharge current intensities ($i=30$ and 40 mA). As examples, experimental relaxation curves, measured in the $2\,^1P$-$4\,^1D$ transition pumping experiment, are compared to the corresponding results given by the identification method for a discharge current intensity $i=40$ mA. In Fig. 3 ($P=3.35$ Torr) and in Fig. 4 ($P=0.37$ Torr). Besides the rather good agreement observed between experimental and calculated curves, Fig. 3 shows that even the $\Delta N_{4^1S}(t)$ and $\Delta N_{4^3S}(t)$ curves are quite well identified despite the small amount of population variation induced on the $4\,^1S$ and $4\,^3S$ states by the $4\,^1D$ state laser perturbation, exhibiting the efficiency of the identification method. Qualitative information on the number of elementary processes leading to the $|i\rangle \rightarrow |j\rangle$ population transfers may already be deduced from the relative positions of relaxation curve maxima. For instance, examination of Fig. 4 indicates that one elementary process is needed for the $4\,^1D \rightarrow 4F$ transfer, two processes for the $4\,^1D \rightarrow 4\,^3D$ one, etc,. This is direct experimental evidence of the previously mentioned major importance of the $4F$ states in collisional redistribution of population between singlet and triplet sublevels. As reported in Eq. (1), one collision transfers population from $4\,^1D$ to $4F$ and another collision transfers population from $4F$ to $4\,^3D$, whereas no direct $4\,^1D \rightarrow 4\,^3D$ process is observed.

No significant dependence on current intensity has been observed for any relaxation curve $\Delta N_i(t)$ or any a_{ij} coefficient. Some a_{ij} coefficients are shown as examples in Fig. 5 for $i=30$ and 40 mA and for the given pressure values. In Eq. (2) one can neglect the contribution of electron-inelastic collisions to excitation transfer and quenching processes of the $n=4$ sublevels. Then the a_{ij} can be written

$$a_{ij} \simeq \alpha_{ij} + n_a \beta_{ij}^P . \tag{19}$$

This result agrees well with previous investigations[1,16,17,19] and with the rate coefficient values proposed by Burrel *et al.*[30]

$$S_{4\,^1P-4\,^1S} = 2.2 \pm 0.7 \times 10^{-5}\ \mathrm{cm^3\,s^{-1}},$$

$$S_{4\,^1P-4\,^3D} = 1.5 \times 10^{-5}\ \mathrm{cm^3\,s^{-1}},$$

($E_e \sim 4.7$ eV) for excitation transfers induced by electronic collisions.

In the same way, similar results are obtained when the $2\,^3P$-$4\,^3D$ and the $2\,^1S$-$4\,^1P$ transitions are optically pumped, the whole giving three independent sets of coefficients a_{ij} as functions of helium pressure. Some of these identification results are summarized as function of P in Fig. 6. A rather good agreement between the results is observed. The α_{ij} and β_{ij} coefficients of Eq. (19) are calculated from the curves $a_{ij}=f(P)$ of Fig. 6 by linear regression. Confidence intervals are obtained through numerical data analysis by varying the experimental points within their error bars. The coefficients α_{ij} are the spontaneous radiative transition probabilities whereas the β_{ij}^P coefficients

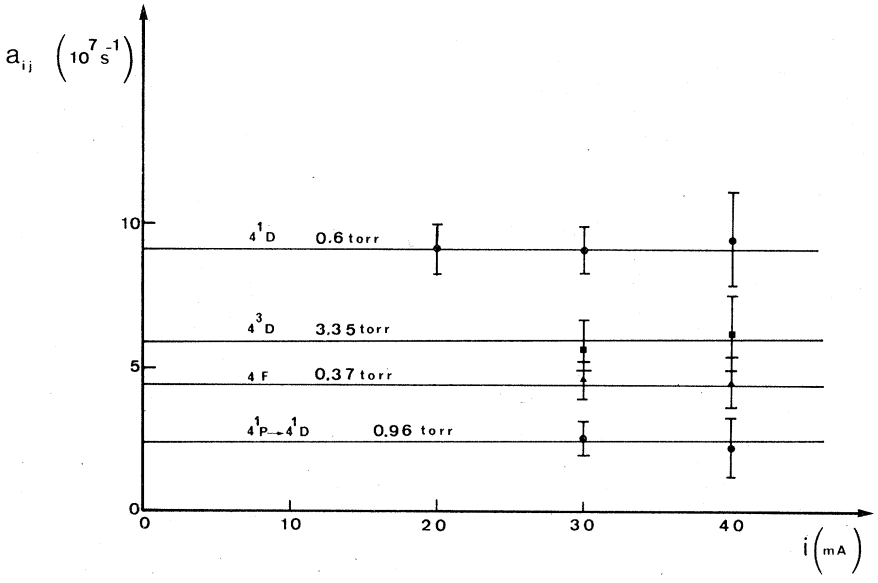

FIG. 5. Some quenching and coupling coefficients of the A matrix as a function of current intensity for various pressure values (Torr).

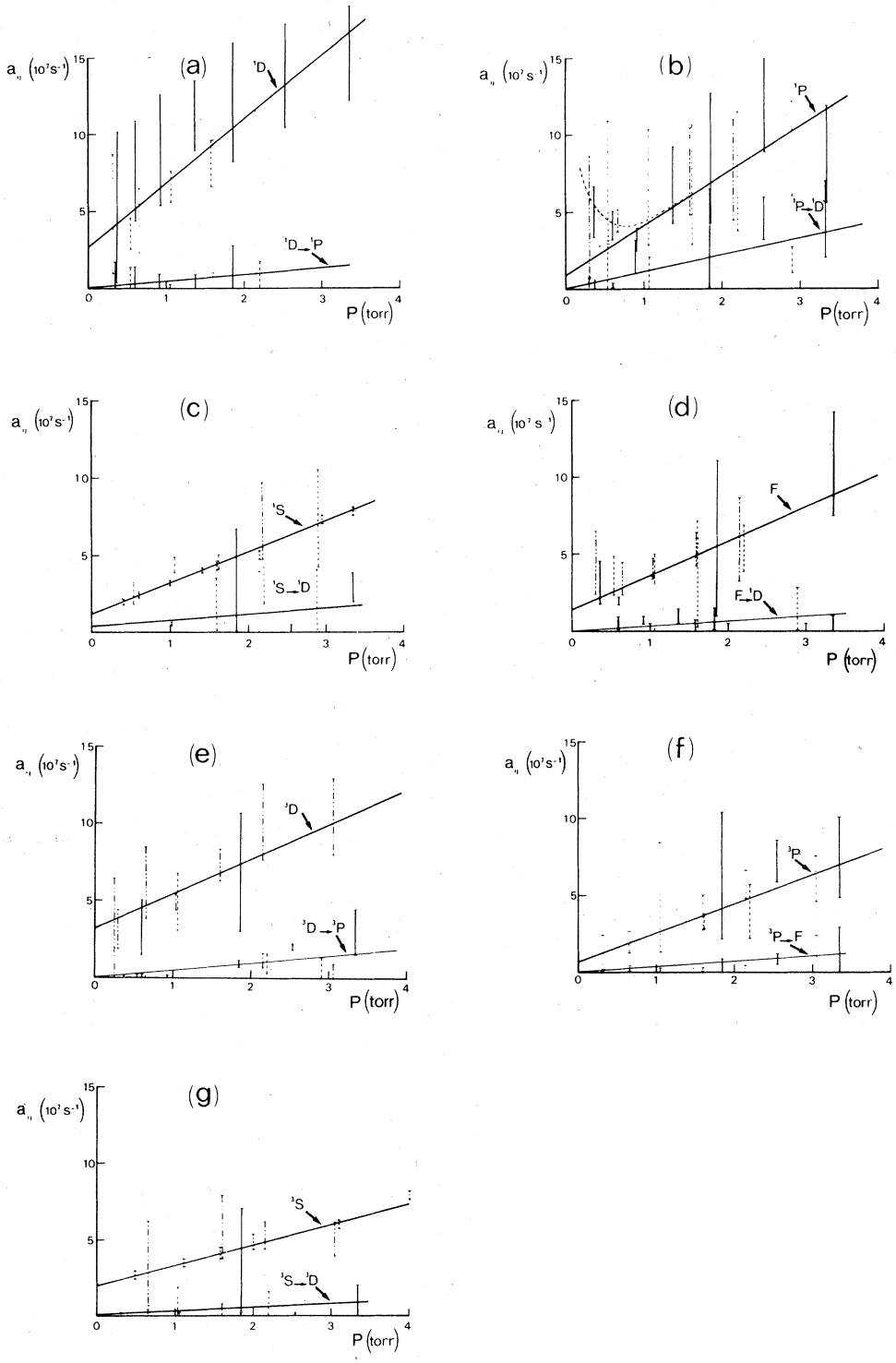

FIG. 6. Some quenching and coupling coefficients of matrix A as functions of helium pressure P: $\mathbf{I}$ the $2\,^1P$-$4\,^1D$ transition is pumped; $\mathbf{\bar{I}}$ the $2\,^1S$-$4\,^1P$ transition is pumped; $\mathbf{\underline{I}}$ the $2\,^3P$-$4\,^3D$ transition is pumped: $\mathbf{\vdots}$ $\Gamma_{4\,1S}$ and $\Gamma_{4\,3S}$ values deduce, respectively, from the $2\,^1P$-$4\,^1S$ and $2\,^3P$-$4\,^3S$ pumping experiments. (a) $a_{11}(^1D)$ and $a_{21}(^1D \rightarrow {}^1P)$; (b) $a_{22}(^1P)$ and $a_{12}(^1P \rightarrow {}^1D)$; (c) $a_{33}(^1S)$ and $a_{13}(^1S \rightarrow {}^1D)$; (d) $a_{44}(F)$ and $a_{14}(F \rightarrow {}^1D)$; (e) $a_{55}(^3D)$ and $a_{65}(^3D \rightarrow {}^3P)$; (f) $a_{66}(^3P)$ and $a_{46}(^3P \rightarrow F)$; (g) $a_{77}(^3S)$ and $a_{57}(^3S \rightarrow {}^3D)$.

are the atom-atom collisional rates. β_{ij}^{P} is related to the corresponding thermally averaged cross sections $\bar{\sigma}_{ij}$ by the relation

$$\bar{\sigma}_{ij} = |\beta_{ij}^{P}| \times (8RT_g/\pi M)^{-1/2}, \quad (20)$$

where R is the ideal gas constant and M is the reduced mass of the colliding partners. The radiative coefficients and the collisional thermally averaged cross sections thus obtained are summarized, respectively, in Tables I and in II.

As in paper I, one can extract further information from the a_{ij} values. Indeed, examination of Table II shows that in numerous cases we have

$$\bar{\sigma}_{ii} \neq \sum_{j \neq i} \bar{\sigma}_{ji}.$$

This difference is due to collisional processes leading to a loss of population from state $|i\rangle$ to states outside the perturbed system [see Eq. (9)]. Since for the eleven states involved in the perturbed system, the lifetimes are always much shorter than the typical diffusion times, the difference

$$\bar{\sigma}_{ii} - \sum_{j \neq i} \bar{\sigma}_{ii} \simeq \bar{\sigma}_{i}^{\text{ion}} \quad (21)$$

may be mainly ascribed to associative ionization processes[25]

$$\text{He}\,|i\rangle + \text{He} \rightarrow \text{He}_2^{+} + \bar{e}. \quad (22)$$

$\bar{\sigma}_{i}^{\text{ion}}$ calculated by Eq. (21) gives at least an extremum value of the actual thermally average cross section of reaction (22).

B. $4\,^1S$ and $4\,^3S$ state population perturbation

As previously quoted in Sec. IV A, weak excitation transfers are detected only for the higher pressure values under study ($P \gtrsim 3$ Torr). Then for $P < 3$ Torr, one can assume with a good approximation that the $\Delta N_4{}^1S$ and $\Delta N_4{}^3S$ population variations decay according to a quasi-exponential relaxation law

$$\Delta N_4{}^i S(t) = \Delta N_4^0{}^i S \exp(-\Gamma_4{}^i S t), \quad i = 1, 3 \quad (23)$$

as shown in Fig. 7 for $P = 1.1$ Torr and $i = 40$ mA. The $\Gamma_4{}^1S$ and $\Gamma_4{}^3S$ coefficients deduced from these two experiments are plotted as a function of P together with the coefficients identified from the experimental data of Sec. V A in Figs. 6(c) and 6(g); rather good agreement is observed.

VI. DISCUSSION AND COMPARISON WITH OTHER WORKS

A. Radiative coefficients

As shown in Table I, the radiative coefficients obtained agree quite well with the tabulated values of Wiese *et al.*[23] and with lifetime measurements performed in helium-electron-beam-interaction[5] and in beam-foil[26] experiments. However a special discussion must be made for the $4\,^1P$ state. Indeed, Fig. 6(b) shows that for $P < 1$ Torr, the total destruction coefficient a_{22} of the $4\,^1P$ state deviates largely from the straight line obtained for higher pressure values. A similar behavior had been observed previously[1,18] for the total

TABLE I. Comparison between measured total radiative destruction rates (α_{ii}) and tabulated values of Wiese *et al.* (Ref. 23), lifetime measurements of Thomson *et al.* (Ref. 5) and beam-foil study of Bukow *et al.* (Ref. 26).

		α_{ii} (This work)	Reference 23	Reference 5	Reference 26
$\sum_J A_4{}^1{}_{D\rightarrow J}$	(10^7 s^{-1})	3.2 ±0.5	2.73 ±0.15	2.44 ±0.2	3.04 ±0.2
$\sum_{J\neq \text{ground state}} A_4{}^1{}_{P\rightarrow J}$	(10^7 s^{-1})	0.84 ±0.08	0.88 ±0.05		
$\sum_J A_{4F\rightarrow J}$	(10^7 s^{-1})	1.6 ±0.3	1.39 ±0.14		1.39 ±0.06
$\sum_J A_4{}^3{}_{D\rightarrow J}$	(10^7s^{-1})	2.8 ±0.4	3.18 ±0.15	3.6 ±1.2	3.1 ±0.1
$\sum_J A_4{}^3{}_{P\rightarrow J}$	(10^7 s^{-1})	0.64 ±0.3	0.65 ±0.07	0.8 ±0.1	
$\sum_J A_4{}^1{}_{S\rightarrow J}$	(10^7 s^{-1})	1.20 ±0.05	1.11 ±0.1	1.12 ±0.05	1.28 ±0.06
$\sum_J A_4{}^3{}_{S\rightarrow J}$	(10^7 s^{-1})	2.0 ±0.2	1.72 ±0.2	1.61 ±0.2	1.61 ±0.07

TABLE II. Measured thermally averaged cross sections for quenching $\bar{\sigma}_{ii}$, excitation transfer $\bar{\sigma}_{ij}$, and associative ionization $\bar{\sigma}_i^{ion}$ in 10^{-15} cm^2 unit. Comparison with previous data: (a) Abrams *et al.* (Ref. 14); (b) Shaw *et al.* (Ref. 7); (c) Glick *et al.* (Ref. 4); (d) Jobe *et al.* (Ref. 3); (e) Kay *et al.* (Ref. 28); (f) Lin *et al.* (Ref. 13); (g) St John *et al.* (Ref. 12); (h) Frish *et al.* (Ref. 29); (i) Cohen (Ref. 33).

(10^{-15} cm^2)	This work	Previous works
$\bar{\sigma}_{4^1D}$	7.7 ±0.4	
$\bar{\sigma}_{4^1P}$	6.3 ±0.9	25 ±2[c]
$\bar{\sigma}_{4^1S}$	3.65 ±0.08	
$\bar{\sigma}_{4F}$	3.9 ±0.4	
$\bar{\sigma}_{4^3D}$	4.5 ±0.5	
$\bar{\sigma}_{4^3P}$	3.6 ±0.3	
$\bar{\sigma}_{4^3S}$	2.40 ±0.07	
$\bar{\sigma}_{4^1D\text{-}4^1P}$	1.0 ±0.2	8.0[b]
$\bar{\sigma}_{4^1P\text{-}4^1D}$	2.1 ±0.6	17[b]; 13[c]; 2.5 ±0.7[h]
$\bar{\sigma}_{4^1D\text{-}4^1S}$	0.35 ±0.08	
$\bar{\sigma}_{4^1S\text{-}4^1D}$	0.3 ±0.3	
$\bar{\sigma}_{4^1D\text{-}4F}$	1.85 ±0.25	9.7 (4^1D-4^1F) and 16 (4^1D-4^3F)[b], 56 $(4D-4F)$[c]
$\bar{\sigma}_{4F\text{-}4^1D}$	0.47 ±0.06	7.1 (4^1F-4^1D) and 3.8 (4^3F-4^1D)[b], 60 ±15 $(4F-4D)$[c], 47 ±15 $(4F-4D)$[d]
$\bar{\sigma}_{4^1P\text{-}4^1S}$	0.95 ±0.05	
$\bar{\sigma}_{4^1S\text{-}4^1P}$	0.28 ±0.12	
$\bar{\sigma}_{4^1P\text{-}4F}$	2.0 ±1.5	12[c], 21 ±5[d], 20[e], ~10[f], 1.2(4^1P-4^3F)[g], 0[b]
$\bar{\sigma}_{4F\text{-}4^1P}$	0.14 ±0.03	9[c], 0.2(4^3F-4^1P)[g], 0[b]
$\bar{\sigma}_{4^1S\text{-}4F}$	0.18 ±0.06	
$\bar{\sigma}_{4F\text{-}4^1S}$	0.10 ±0.03	
$\bar{\sigma}_{4^3D\text{-}4F}$	0.66 ±0.13	5.1 (4^3D-4^1F) and 14 (4^3D-4^3F)[b]
$\bar{\sigma}_{4F\text{-}4^3D}$	0.35 ±0.04	1.1 (4^1F-4^3D) and 10 (4^3F-4^3D)[b]
$\sigma_{4^3P\text{-}4F}$	0.30 ±0.13	0[b]
$\bar{\sigma}_{4F\text{-}4^3P}$	0.20 ±0.05	0[b]
$\bar{\sigma}_{4F\text{-}4^3S}$	0.10 ±0.05	
$\bar{\sigma}_{4^3S\text{-}4F}$	0.01 ±0.01	
$\bar{\sigma}_{4^3D\text{-}4^3P}$	0.88 ±0.16	
$\bar{\sigma}_{4^3P\text{-}4^3D}$	0.58 ±0.13	0.99 ±0.24[a], 8.1[b]
$\bar{\sigma}_{4^3D\text{-}4^3S}$	0.35 ±0.03	
$\bar{\sigma}_{4^3S\text{-}4^3D}$	0.07 ±0.07	
$\bar{\sigma}_{4^3P\text{-}4^3S}$	0.29 ±0.03	0.35 ±0.03[a]
$\bar{\sigma}_{4^3S\text{-}4^3P}$	0.03 ±0.02	
$\bar{\sigma}^{ion}_{4^1D}$	4.5 ±2.1	5.6[b]
$\bar{\sigma}^{ion}_{4^1P}$	1.3 ±1.3	9.4[b]
$\bar{\sigma}^{ion}_{4^1S}$	1.9 ±1.5	
$\bar{\sigma}^{ion}_{4F}$	2.5 ±0.6	4 (4^1F) and 1.3 (4^3F)[b]
$\bar{\sigma}^{ion}_{4^3D}$	2.6 ±0.8	1.9[b], 0.431[i]
$\bar{\sigma}^{ion}_{4^3P}$	2.4 ±0.7	3.1[b], 0.166[i] (T_g = 300 K)
$\bar{\sigma}^{ion}_{4^3S}$	2.1 ±0.2	0.06[i] (T_g = 300 K)

[a] Reference 14.
[b] Reference 7.
[c] Reference 4.
[d] Reference 3.
[e] Reference 28
[f] Reference 13.
[g] Reference 12.
[h] Reference 29.
[i] Reference 33.

quenching rate coefficient of the $3\,^1P$ helium state. As reported, this result is quite suggestive of the escape of radiation in the $4\,^1P$-$1\,^1S$ resonant transition ($\Lambda_{4^1P\text{-}1^1S} \neq 0$) for the lower pressure values, which is on the contrary entirely trapped ($\Lambda_{4^1P\text{-}1^1S} \cong 0$) for $P > 2$ Torr. A detailed study of this mechanism has been made in Ref. 17 for the 3^1P state and results agree quite well with radiative transfer theoretical calculations.[27] Finally, note that all the radiative rate coefficients between each pair of $n=4$ sublevels are found negligibly small at measurement accuracy.

B. Collisional coefficients

The excellent agreement between the results obtained in the five independent experiments represents an important check on the coherence and accuracy of the experimental and numerical method. As a supplementary check of our thermally averaged cross-section values, we have compared the ratios $\bar{\sigma}_{ij}/\bar{\sigma}_{ji}$ to their theoretical values given by the microreversibility principle. As reported in Table III, agreement is quite good while the $\bar{\sigma}_{ij}$ values are obtained without any

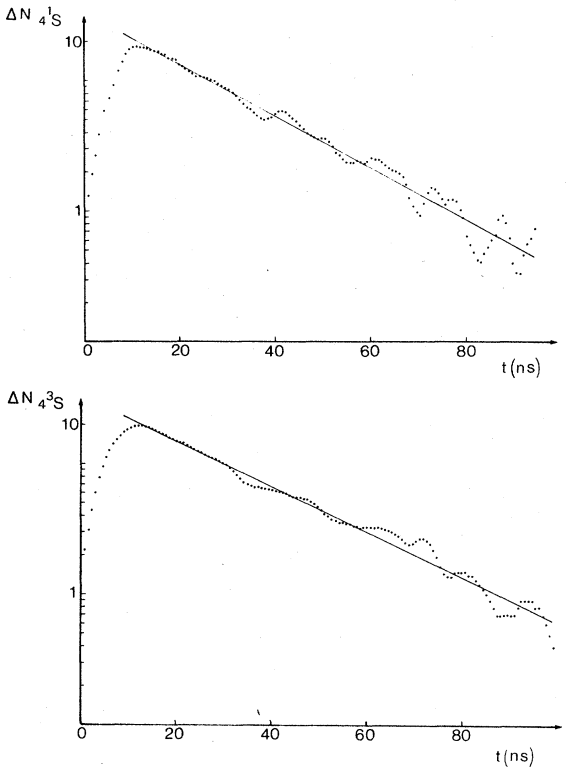

FIG. 7. Measured population relaxations $\Delta N_{4\,^1S}(t)$ and $\Delta N_{4\,^3S}(t)$ in arbitrary units and semilogarithmic scale for $P=1$, 1 Torr, and $i=40$ mA.

"a priori" assumption. Coming back to Fig. 6(c) one can observe that the $a_{13}=f(P)$ curve ($4^1S \rightarrow 4^1D$ transfer) does not intercept the vertical axis at the origin. This remaining contribution to the 4^1S-4^1D transfer extrapolated at zero pressure value is interpreted as being due to non-negligible excitation transfers induced by electronic collisions with a corresponding rate coefficient of about 3×10^{-5} cm^3 s^{-1}. This value is found to be of the same order of magnitude that the rate coefficient $S_{4^1P-4^1S}=2.2\pm0.7\times10^{-5}$ cm^3 s^{-1} measured by Burrel *et al.*[30] in an electron-beam-created helium plasma ($E_e=4.7$ eV).

TABLE III. Comparison between experimental ratios $\bar{\sigma}_{ij}/\bar{\sigma}_{ij}$ and calculated values using the microreversibility principle.

	This work	Microreversibility
$\bar{\sigma}_{4^1D-4^1P}/\bar{\sigma}_{4^1P-4^1D}$	0.476 ±0.2	0.493
$\bar{\sigma}_{4^1D-4^1S}/\bar{\sigma}_{4^1S-4^1D}$	1.25 ±1.25	1.7
$\bar{\sigma}_{4^1D-4F}/\bar{\sigma}_{4F-4^1D}$	0.254 ±0.07	0.183
$\bar{\sigma}_{4^1P-4^1S}/\bar{\sigma}_{4^1S-4^1P}$	3.39 ±1.6	3.45
$\bar{\sigma}_{4^1P-4F}/\bar{\sigma}_{4F-4^1P}$	14 ±10	11
$\bar{\sigma}_{4^1S-4F}/\bar{\sigma}_{4F-4^1S}$	0.55 ±0.35	0.31
$\bar{\sigma}_{4^3D-4F}/\bar{\sigma}_{4F-4^3D}$	0.53 ±0.16	0.55
$\bar{\sigma}_{4^3P-4F}/\bar{\sigma}_{4F-4^3P}$	0.67 ±0.3	0.87
$\bar{\sigma}_{4F-4^3S}/\bar{\sigma}_{4^3S-4F}$	10. ±10	14
$\bar{\sigma}_{4^3D-4^3P}/\bar{\sigma}_{4^3P-4^3D}$	1.51 ±0.6	1.56
$\bar{\sigma}_{4^3D-4^3S}/\bar{\sigma}_{4^3S-4^3D}$	≥ 5	25.5
$\bar{\sigma}_{4^3D-4^3S}/\bar{\sigma}_{4^3S-4^3P}$	9.7 ±8	16.3

Our results are compared to previous measurements in Table II. Large discrepancies are observed especially with investigations performed in helium-electron-beam-interaction experiments[3,4,12,13,28,29] whereas good agreement is found with Abrams *et al.*[14] for the two thermally averaged cross sections they have measured by means of a selective laser-perturbation technique. Indeed in helium-electron-beam-interaction experiments, great difficulties arise in the determination of individual cross section of a selected reaction channel due to the nonselectivity of the initial perturbation. Furthermore, as clearly discussed by some authors[3,4] further obstacles arise from the contribution of numerous processes such as radiation trapping, collisional and radiative cascades from higher levels and excitation transfers induced by low-energy secondary electrons. Moreover, Burrel *et al.*[30] suggest that the large values (some 100 Å^2) measured in these helium-electron-beam-experiments may be ascribed to reactions of the type

$$\begin{aligned} &\mathrm{He}(4\,^1D)+\mathrm{He}(1\,^1S)\rightarrow \mathrm{He}(4F)+\mathrm{He}(1\,^1S)\,,\\ &\mathrm{He}(4F)+\bar{e}\rightarrow \mathrm{He}(4\,^3D)+\bar{e}\,. \end{aligned} \tag{24}$$

Then no concluding remarks can be infered from the comparison of our results with those obtained from nonselective methods due to the fact that, besides the difficulties connected with the determination of absolute cross sections in these experiments, one does not actually know what contributions are contained in the proposed values.

On the other hand, the results obtained from selective perturbation experiments can be more directly compared with our measurements. Indeed, a quite good agreement is observed, as previously mentioned, with results proposed in Ref. 14. On the contrary, a large discrepancy is observed with the cross-section values proposed by Shaw *et al.*[7] though they use a similar experimental technique. However, several reasons can explain these disagreements. Indeed, the cross sections of Ref. 7 are only deduced from time resolved (resolution 10 ns) measurements of fluorescence light intensities induced in the $4\,^1P$-$2\,^1S$ and $4\,^3D$-$2\,^3P$ transitions when the $4\,^1D$ state is perturbed by laser optical pumping of the $2\,^1P$-$4\,^1D$ transition in an afterglow. Since the number of unknowns is larger than the number of measurements, the solution of such a problem is not unique

and requires several assumptions. The model is selected to give the best fit of the two experimental curves assuming that forward and backward cross sections are connected by the microreversibility principle and that the only efficient excitation transfers agree with Wigner spin conservation rules for the $L < 3$ sublevels and with the selection rule $\Delta L = \pm 1$. This last assumption is not supported theoretically and is not confirmed in the other experiments. Moreover, the authors do not give any error bars for their results since, as said in Ref. 7, there is no guarantee that the optimum model is a good representation of reality. Then no direct comparison with our results can be achieved.

In order to explain the measurement of St. John *et al.*,[12] Lin *et al.*[13] have suggested the selection rule $\Delta L = \pm 2$ though excitation transfer with $\Delta L = \pm 1$ and $\Delta L = \pm 3$ may weakly contribute in helium atom-atom collisions. As one can observe in Table II, no strict selection rule on the orbital quantum number changing can be isolated from the results, at least for excitation transfers involving states if the energy gap ΔE between them is lower than the mean kinetic energy of atoms (kT_g). The thermally averaged cross-section values $\bar{\sigma}_{ij}$ mainly depend on ΔE as shown in Fig. 8 where we have summarized the present results and those previously obtained in paper I and in paper II as a function of the dimensionless ratio $\Delta E/kT_g$. It is noticeable that the cross-section values are distributed along a regular curve similar to the one proposed by Stuckelberg[31] for low energy quasiresonant collisions between excited and ground-state atoms. On the contrary, differences are observed as a function of ΔL for excitation transfers with $\Delta E > kT_g$: $4\,^1S \rightleftarrows |j\rangle$ and $4\,^3S \rightleftarrows |j\rangle$. This last point can only be explained in terms of relative positions of interaction potential curve crossings and relative values of potential humps and atomic kinetic energy in a collision.[32]

To our knowledge, the only theoretical cross-section values for the $n = 4$ helium sublevels have been proposed by Cohen[33] and concerns the associative ionization of the $4\,^3S$, $4\,^3P$, and $4\,^3D$ states. As shown in Table II, they are found much smaller than the measured ones whereas for the $3\,^3S$, $3\,^3P$, and $3\,^3D$ the agreement is quite good as reported in paper I. The observed discrepancy may be ascribed on one hand to the fact that the measured $\bar{\sigma}_i^{\text{ion}}$ of Table II just represent a maximum value of the actual associative ionization cross section as previously quoted (Eq. (21), and on the other hand to the simplification performed in the theoretical calculation. Specifically long-range couplings have not been taken into account

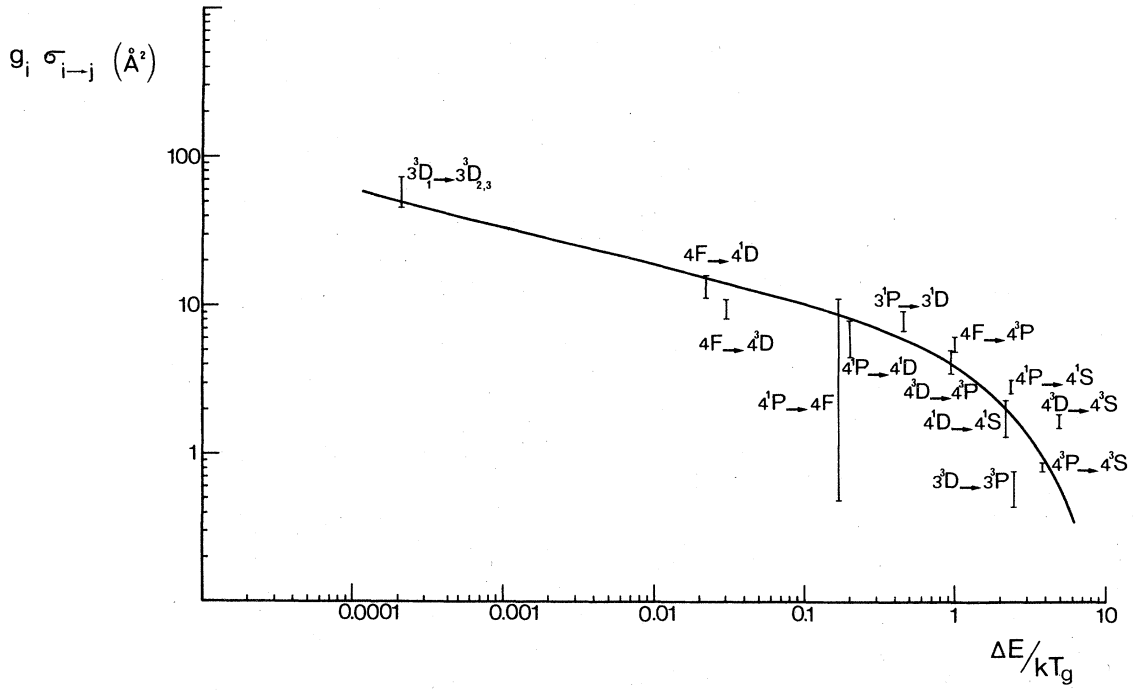

FIG. 8. Excitation transfer thermally averaged cross sections as a function of the dimensionless ratio $\Delta E/kT_g$. The $n = 3$ values are taken from paper I and paper II.

despite their possible large contribution for states with principal quantum number $n > 4$ as reported in Ref. 33.

VII. CONCLUSION

The quenching and excitation transfer mechanisms in the $n=4$ helium sublevels have been studied in a glow discharge by the same procedure as in paper I and in paper II. The results show that even for this complicated system (seven states interact), all the coupling coefficients between each state pair can be determined with a rather good accuracy, good guarantees of validity and a threshold of detection as small as $\bar{\sigma} \sim 5 \times 10^{-17}$ cm^2. The measured radiative destruction rates agree well with accepted values. The excitation-transfer cross-section values obtained clearly indicate that Wigner spin conservation rules hold for atom-atom binary encounter involving ($n=4$, $L < 3$) helium sublevels and that the observed singlet-triplet excitation transfers are due to stepwise processes via the $4F$ state. On the other hand, examination of Table II shows that no strict selection rules on L-number changing collisions can be deduced from measurements but the thermally averaged cross-section values obtained agree rather well with the quasiresonant low-energy collision theory of Stuckelberg.[31] Finally, the present work demonstrates that the laser-perturbation technique associated with the identification method of data analysis now allows us to consider complex interactive systems.

[1] B. Dubreuil and A. Catherinot, Phys. Rev. A 21, 188 (1980)
[2] A. Catherinot, B. Dubreuil, and G. Gousset, Phys. Rev. A 21, 618 (1980).
[3] J. D. Jobe and R. M. St. John, Phys. Rev. A 5, 295 (1972).
[4] D. E. Lott III, R. E. Glick, and J. A. Llewellyn, J. Quant. Spectros. Radiat. Transfer, 15, 513 (1975); P. H. Wine and R. E. Glick, *ibid.* 16, 879 (1976).
[5] R. T. Thompson and R. G. Fowler, J. Quant. Spectros. Radiat. Transfer. 15, 1017 (1975).
[6] C. F. Burrel and H. J. Kunze, Phys. Rev. Lett. 28, 1 (1972).
[7] M. J. Shaw and M. J. Webster, J. Phys. B 9, 2839 (1976).
[8] A. Catherinot, B. Dubreuil, A. Bouchoule, and P. Davy, Phys. Lett. 56A, 469 (1976); A. Catherinot and B. Dubreuil, Orléans, Report No. 76/01, 1976 (unpublished).
[9] E. Wigner, *Nachrichten von der Gesellschaft der Wissenschaften zu Göttingen* (Weidmannische Buchhandlung, Berlin, 1927), p. 375.
[10] J. H. Lees and H. W. B. Skinner, Proc. R. Soc. London 137A, 186 (1932).
[11] W. Maurer and R. Wolf, Z. Phys. 92, 100 (1934); R. Wolf and W. Maurer, *ibid.* 115, 410 (1940).
[12] R. M. St. John and R. G. Fowler, Phys. Rev. 122, 1813 (1961).
[13] C. C. Lin and R. G. Fowler, Ann. Phys. (N.Y.) 15, 461 (1961).
[14] R. L. Abrams and G. J. Volga, Phys. Rev. Lett. 19, 1411 (1967).
[15] R. K. Van Den Eynde, G. Wiedes, and T. Niemeyer, Physica (Utrecht) 59, 401 (1972).
[16] B. Dubreuil, thesis Orléans, 1979 (unpublished).
[17] A. Catherinot, thesis Orléans, 1980 (unpublished).
[18] B. Dubreuil and A. Catherinot, Physica (Utrecht) C93, 408 (1978).
[19] B. Dubreuil and A. Catherinot, J. Phys. D 11, 1043 (1978).
[20] A. Catherinot, B. Dubreuil, and M. Gand, Phys. Rev. A 18, 1097 (1978); B. Dubreuil and A. Catherinot, J. Phys. (Paris) 39, 1071 (1978).
[21] A. Catherinot, P. Placidet, and B. Dubreuil, J. Phys. B 11, 3775 (1978).
[22] A. Catherinot and A. Sy, Phys. Rev. A 20, 1511 (1979).
[23] W. L. Wiese, H. W. Smith, and B. M. Glennon, Natl. Stand. Ref. Data Ser., Natl. Bur. Stand. 1, 4 (1966).
[24] Note that the $4\,^3P$ state population is never directly laser perturbed.
[25] J. Stevefelt and F. Robben, Phys. Rev. A 5, 1502 (1972).
[26] H. H. Bukow, G. Heine, and H. Reinke, J. Phys. B 10, 2347 (1977).
[27] F. E. Irons, J. Quant. Spectros. Radiat. Transfer 22, 1 (1979).
[28] R. B. Kay and R. H. Hughes, Phys. Rev. 154, 61 (1967).
[29] S. E. Frish and Y. E. Ionikh, Opt. Spectrosc. 25, 91 (1968) [Opt. Spektrosk. (USSR) 25, 171 (1968)].
[30] C. F. Burrel and H. J. Kunze, Phys. Rev. A 18, 2081 (1978).
[31] E. C. G. Stueckelberg, Helv. Phys. Acta 5, 370 (1932).
[32] J. S. Cohen, Phys. Rev. A 13, 86 (1976).
[33] J. S. Cohen, Phys. Rev. A 13, 99 (1976).